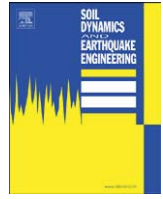




Contents lists available at ScienceDirect

Soil Dynamics and Earthquake Engineering

journal homepage: www.elsevier.com/locate/soildyn

Fragility curves for expressway embankments based on damage datasets after recent earthquakes in Japan

Yoshihisa Maruyama^{a,*}, Fumio Yamazaki^a, Kiku Mizuno^b, Yoshiyuki Tsuchiya^c, Hiroyuki Yogai^c

^a Department of Urban Environment Systems, Chiba University, 1-33 Yayoi-cho, Inage-ku, Chiba 263-8522, Japan

^b East Japan Railway Company, Co., Ltd., Japan

^c Nippon Expressway Research Institute, Co., Ltd., Japan

ARTICLE INFO

Article history:

Received 2 September 2009

Received in revised form

19 April 2010

Accepted 27 April 2010

ABSTRACT

The seismometer network of the Japanese expressway system was enhanced following the 1995 Kobe earthquake. Based on earthquake information from the instruments of the seismometer network, a traffic control is performed directly after the event because of the potential for damage to expressway structures. Expressways serve as vital trunk lines of transportation and are important for the restoration of damage-stricken areas. Therefore, earthquake-induced damage to expressway structures should be estimated as soon as possible. Expressway embankments were seriously damaged during recent earthquakes, such as the 2004 Niigata Chuetsu earthquake. The present study constructs the fragility curves of expressway embankments in Japan in order to estimate the damage distribution immediately after an earthquake. Damage datasets for expressways are compiled for the 2003 Northern-Miyagi earthquake, the 2003 Tokachi-oki earthquake, the 2004 Niigata Chuetsu earthquake, and the 2007 Niigata Chuetsu-oki earthquake. The spatial distributions of the peak ground velocity (PGV) are estimated for these four earthquakes in order to evaluate the relationship between the damage ratio of expressway embankments and the PGV. Statistical analysis is then conducted in order to draw the fragility curves for expressway embankments. Based on the fragility curves, major damage that disrupts ordinary expressway traffic may occur when the peak ground velocity exceeds approximately 35.0 cm/s. The fragility curves constructed in the present study are helpful for predicting the damage distribution on expressways soon after an earthquake, which enables efficient traffic control and rapid disaster response.

© 2010 Elsevier Ltd. All rights reserved.

1. Introduction

After the 1995 Kobe earthquake, a higher priority has been given to countermeasures against earthquakes in Japan. With the help of good financing, thousands of strong motion seismometers were installed in Japan [1–2]. In addition, a number of damage assessment systems have been developed by different organizations [3]. Under these circumstances, a new seismometer network has been developed along expressways. Using earthquake information obtained from these instruments, a traffic control is performed directly after the event because of the potential damage to expressway structures [4].

Expressway structures in Japan were severely damaged during the 1995 Kobe earthquake. This event damaged numerous highway bridges. Collapse and near collapse occurred at nine sites, and other damage occurred at 16 sites [5]. During this event, elevated bridges in urban areas suffered extensive damage for the

first time in Japan. Currently, the fragility curves of expressway structures in Japan are constructed empirically [6] and analytically [7–8] based on lessons learned from the Kobe earthquake. Fragility curves are regarded as useful tools for estimating the extent of probable damage (slight, moderate, extensive, and complete) of structures due to an earthquake [9–11].

Expressway embankments have also been seriously damaged during recent earthquakes. Damage resulting from the Niigata Chuetsu earthquake ($M_w=6.7$) [12], which occurred on October 23, 2004, primarily affected the embankment sections of the Kan'etsu and Hokuriku Expressways. Three large-scale collapses of expressway embankments occurred in areas that experienced severe seismic motion. A traffic control was carried out, and the expressway was tentatively reopened on November 5. The four-lane roadway was opened to regular traffic after approximately 1 month.

The expressway network serves as the trunk line of transportation and is important to the restoration of damage-stricken areas. As such, the severity of damage to these structures should be estimated at an early stage based on the ground motion indices obtained by

* Corresponding author. Tel.: +81 43 290 3555; fax: +81 43 290 3558.
E-mail address: ymaruyam@tu.chiba-u.ac.jp (Y. Maruyama).

seismometers along the expressways. In order to achieve this objective, the present study constructs fragility curves of expressway embankments using actual damage datasets for recent earthquakes in Japan. The spatial distributions of the peak ground velocities (PGV) are estimated by the simple Kriging method with a trend component, and the relationships between the PGVs and the damage ratios of expressway embankments are investigated in order to obtain the fragility curves. Generally speaking, the peak ground acceleration (PGA) strongly depends on high frequency contents of ground motion, which differs from site to site. On the contrary, the peak ground displacement (PGD) represents long period contents of seismic motion, which are less correlated to embankment damages. Since the PGV and the spectral intensity (SI) are not so sensitive to high frequency contents and they are considered to represent the energy of the medium-period range motion, which has higher correlation with embankment damages, the distribution of the PGV is adopted to show the intensity of seismic motion in this study.

2. Dataset of expressway damage following recent earthquakes

Table 1 describes the severity of the damage as defined by Nippon Expressway Company, Co., Ltd. (NEXCO). Five levels, namely, severe (As), major (A), moderate (B), minor (C), and very minor (D), were used to categorize the damage to the expressway. The damage levels are defined for different types of expressway components, including bridge superstructures, substructures, load-bearing structures, and tunnels. The damage associated with damage levels As, A, and B was severe enough to disrupt ordinary expressway traffic.

Four recent earthquakes that damaged expressways in Japan are considered in the present study: the 2003 Northern-Miyagi earthquake ($M_w=6.2$), the 2003 Tokachi-oki earthquake ($M_w=8.3$), the 2004 Niigata Chuetsu earthquake, and the 2007 Niigata Chuetsu-oki earthquake ($M_w=6.6$) [13]. The damage caused by these events was classified into five levels, as shown in Table 1. Fig. 1 shows examples of damage to embankments following the 2004 Niigata Chuetsu earthquake. Large-scale collapses of the side slope, which are classified as level A damage, were observed along the Kan'etsu Expressway. The damage is recorded with respect to the kilometer post (KP) with the intervals of 10 m. If different components of the expressway

were damaged at the same KP, all of the damage was recorded in the damage datasets.

Fig. 2 shows the number of individual damage incidents to expressways following the 2004 Niigata Chuetsu earthquake. The figure includes only level A and level B damage. No level As damage were observed during this event. According to the figure, approximately 65% of the incidents involved damage to roadways and side slopes. Damage to bearing structures and bridge superstructures account for approximately 25% of the total number of incidents. The remaining incidents consisted primarily of deformations of box culverts. Since all four of the earthquakes considered herein caused more damage to roadways and side slopes than to bridges, the present study focuses on the relationship between the intensity of the ground motion and the damage ratio of the expressway embankment. In Japan, expressways occupy mountainous regions in rural areas. Therefore, evaluation of the seismic performance of expressway embankments is desired in order to enable rapid restoration work in rural areas.

3. Spatial distributions of peak ground velocity

In order to evaluate the relationship between the seismic intensity and the damage ratio of the expressway embankment, the seismic intensity at the site where the damage occurred should be properly considered. The ground motion distribution can be estimated by attenuation relationships that express the source, path, site effects, and, occasionally, the influence of other variables [14–16]. However, ground motion distributions are greatly affected by the local site and subsurface geological conditions.

The shear wave velocity averaged over the upper 30 m (V_s^{30}) is used as an appropriate simplified site conditions term [17]. Based on V_s^{30} and the classification of geologic units, maps of region-wide site conditions were constructed for California [18]. Matsuoka and Midorikawa [19] developed a GIS-based amplification map for the Tokyo metropolitan area. Yamazaki et al. [20] proposed a method by which to estimate amplification ratios for strong ground motion parameters that is applicable to all of Japan. These studies used the Digital National Land Information (DNLI) of Japan as geomorphological and geological information, which is presented as a standard $1 \times 1 \text{ km}^2$ mesh.

Table 1
Severity of damage to the expressway structures in Japan.

Damage	Severe (As)	Major (A)	Moderate (B)	Minor (C)	Very minor (D)
Bridge superstructure	Collapse	Large lateral displacement, but no collapse Rupture of steel girder	Deformation or buckling of steel girder	Deformation of bridge joint	
Bridge substructure	Failure of bridge pier	Rupture of reinforcement	Large detachment or crack in cover concrete Exposure of reinforcement	Small detachment or crack in cover concrete Small detachment or crack in cover concrete	
Bearing structure		Rupture of bearing Rupture of anchor bolt	Large detachment or crack in cover concrete Shear deformation of bearing Rupture of concrete	Partial damage to bearing Crack in concrete or anchor bolt Breakaway of anchor bolt	Loose anchor bolt
Tunnel		Rupture of lining	Large detachment or crack in lining	Small detachment or crack in lining	
Side slope		Total collapse	Partial collapse	Deformation	
Gap in roadway			Traffic lane: more than 3 cm Shoulder: more than 20 cm	Traffic lane: 1–3 cm Shoulder: 1–20 cm	Less than 1 cm
Crack in roadway			More than 5 cm	3–5 cm	Less than 3 cm



Fig. 1. Typical damage to expressway embankments after the 2004 Niigata Chuetsu earthquake.

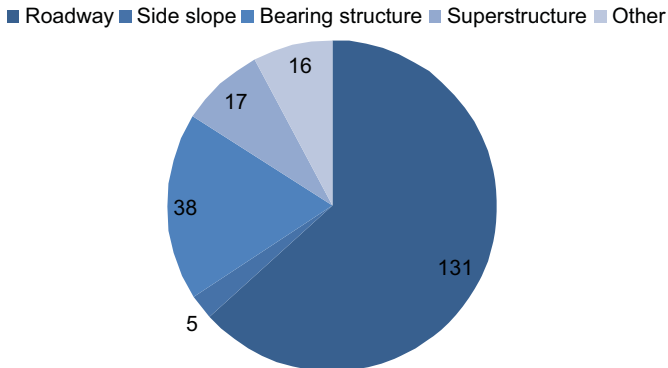


Fig. 2. Number of damage incidents for different components of expressways after the 2004 Niigata Chuetsu earthquake. Only level A and level B damage incidents are illustrated.

Wakamatsu et al. [21] proposed the Japan Engineering Geomorphologic Classification Map (JEGM) based on a new engineering-based geomorphologic classification scheme because the DNLI often uses different geomorphologic classifications that vary according to prefecture. Recently, they extended JEGM, which currently consists of $250 \times 250 \text{ m}^2$ grid cells. The grid cells are categorized by geomorphologic characteristics into 24 classes. A nationwide V_s^{30} distribution map is created using the nationwide shear wave velocity datasets for Japan, which are available from K-NET (approximately 1,000 sites) and KiK-net [2] (approximately 500 sites) survey sites, and JEGM [22]. Considering the relationship between V_s^{30} and the amplification factor of the peak ground velocity (PGV) [23], a nationwide map of amplification factors is obtained. The amplification factors are defined with respect to the outcrop base with a shear wave

velocity of 600 m/s. Fig. 3 shows the amplification factors map used in the present study. The epicenters of the four earthquakes are also illustrated in the figure.

Fig. 4 shows a schematic diagram for the interpolation of the PGV performed in the present study. Simple Kriging [24], which is a method of stochastic interpolation, is used to draw the spatial distribution. We applied the simple Kriging technique assuming a prior trend component, because the underlying random function model is the sum of trend and residual components [25]:

$$Z(u) = m(u) + R(u) \quad (1)$$

where $Z(u)$ is the random variable model at location u , $m(u)$ is the trend component, which is modeled as a smoothly varying deterministic function of the coordinate vector u , and $R(u)$ is the residual component modeled as a stationary random function with a zero mean and covariance.

The trend component (deterministic function) is assigned for the attenuation relationship obtained at the outcrop base. In order to obtain the attenuation relationship at the base, the recorded PGV is first deconvoluted to the outcrop base. Although the amplification factors in Fig. 3 are used in deconvolution, they are assigned as the averaged values of $250 \times 250 \text{ m}^2$ pixels. If more detailed amplification factors are available, the use of these datasets is more desirable. Shabestari and Yamazaki [26] constructed the following attenuation relationship of the PGV using K-NET accelerometer records:

$$\log_{10} PGV = b_0 + b_1 M + b_2 r - \log_{10} r + b_4 h + c \quad (2)$$

where b_0 , b_1 , b_2 , and b_4 are regression coefficients, r is the shortest distance from the fault, h is the depth of the hypocenter, and c is the station coefficient. The station coefficients result from geological and topographical site effects. Tamura et al. [27] developed the following relationship between the shear wave velocity averaged over the upper 20 m (V_s^{20}) and the station

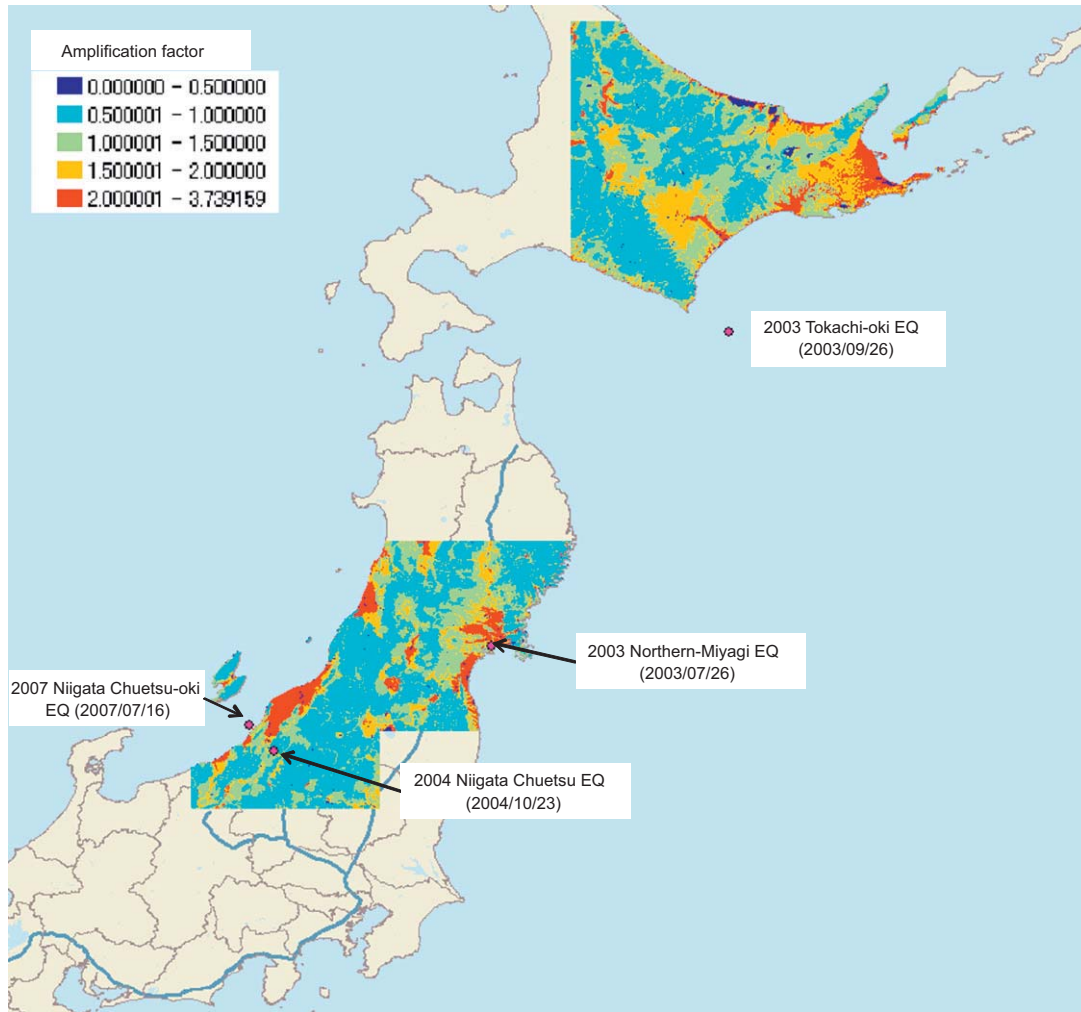


Fig. 3. Amplification factors of the PGV with respect to the outcrop base with a 600 m/s shear wave velocity and the epicenters of the four earthquakes.

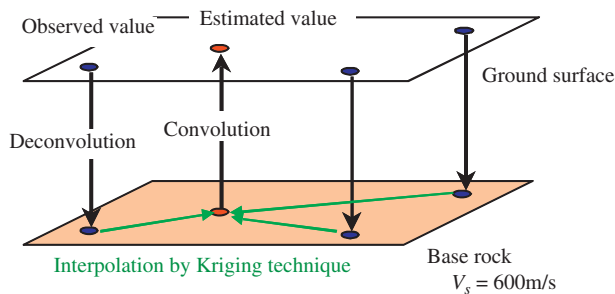


Fig. 4. Schematic diagram for interpolation of the peak ground velocity.

coefficient using approximately 800 PS-logging data for K-NET sites:

$$c = -0.734 \log_{10} V_s^{20} + 1.81. \quad (3)$$

Since the base outcrop is assumed to have a uniform shear wave velocity of 600 m/s, Eq. (3) is adjusted such that $c_r=0$ when $V_s^{20}=600$ m/s. Note that the amplification factor of the PGV with respect to the outcrop base is denoted as 10^{c_r} , where

$$c_r = -0.734 \log_{10} V_s^{20} + 2.04. \quad (4)$$

For the PGV recorded by other instruments, e.g., instruments deployed by JMA and NEXCO, the amplification factors shown in Fig. 3 are used for deconvolution.

The attenuation relationship of the PGV at the outcrop base is then constructed. The fault models developed by the Geographical Survey Institute of Japan [28] for the four earthquake events are considered in the present study. The residual component is defined as the difference between the PGV converted to the base level and the corresponding mean trend component (attenuation relationship) values:

$$R(u) = PGV_{bi} - PGV_{mi} \quad (i = 1, \dots, n) \quad (5)$$

where the suffixes b and m represent the ground motion value at the base and the mean attenuation value, respectively, for n observations.

The residual component is interpolated by simple Kriging. In the Kriging technique, a spatial auto-correlation function should be assigned. An exponential function was used in the present study. The correlation distance, which controls the influence of observed data, is assumed to be 5.0 km [25]. Note that if the correlation distance is large, the estimated distribution connects the observed points irrespective of the trend component, whereas if the correlation distance is small, the estimated distribution approaches the trend rapidly. Since the correlation distance is difficult to be determined from non-dense seismic recordings and it varies from event to event, we assumed the fixed value based on the previous research [6,25].

The strong motion indices at the base are estimated by adding the trend component to the interpolated random component. Multiplying the amplification factors by the values obtained at the

base, the spatial distribution at the ground surface is obtained. Through this method, observed values are obtained for the meshes that include the observation points.

The accuracy of the interpolation method is discussed through the 2004 Niigata Chuetsu earthquake. Only PGVs recorded by K-NET accelerometers are used to estimate the spatial

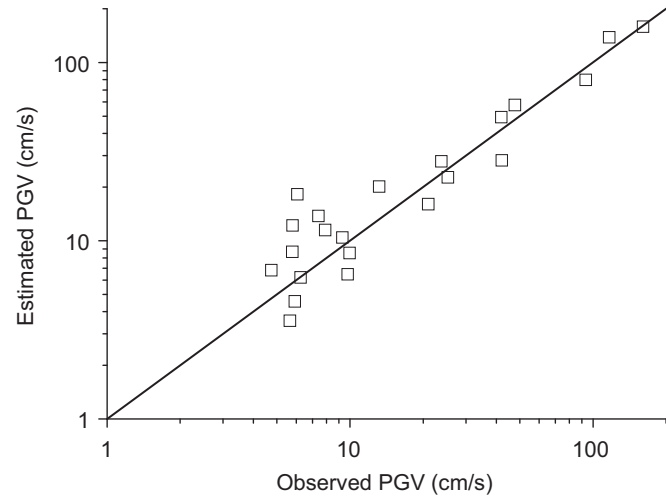


Fig. 5. Comparison between estimated and observed PGVs for the 2004 Niigata Chuetsu earthquake.

distribution, and the estimated values for the sites at which the seismometers deployed by JMA and NEXCO are installed are compared with the recorded values (Fig. 5). The estimated PGV is fairly accurate when the PGV is greater than 20.0 cm/s. Since expressway embankments will be seriously damaged at larger PGVs, the Kriging interpolation used in the present study is expected to provide reasonable spatial distributions of the PGV with which to construct fragility curves.

In the present study, detailed spatial distributions of PGV along the expressways are needed. Therefore, the PGVs obtained by NEXCO seismic observation stations were also used for the Kriging interpolation. Fig. 6 shows the attenuation relationship at base rock (trend component), the estimated PGV distribution, and the PGVs extracted along the Kan'etsu Expressway (from Muikamachi IC to Nagaoka IC) for the 2004 Niigata Chuetsu earthquake. A total of 193 records were used for interpolation. If the PGVs recorded at the ICs are used, the estimated values are changed slightly near the Koide and Echigo-Kawaguchi ICs. The PGV distribution with NEXCO records is expected to show better accuracy than that without NEXCO records because more observed values along the expressways are used for Kriging interpolation.

Fig. 7 shows the estimated PGV distributions for the 2003 Northern-Miyagi, 2003 Tokachi-oki, and 2007 Niigata Chuetsu-oki earthquakes. The PGVs of the 2003 Tokachi-oki (88 records) and 2007 Niigata Chuetsu-oki (88 records) earthquakes were estimated following the same procedures as those for the 2004 Niigata Chuetsu earthquake. With respect to the 2003 Northern-Miyagi

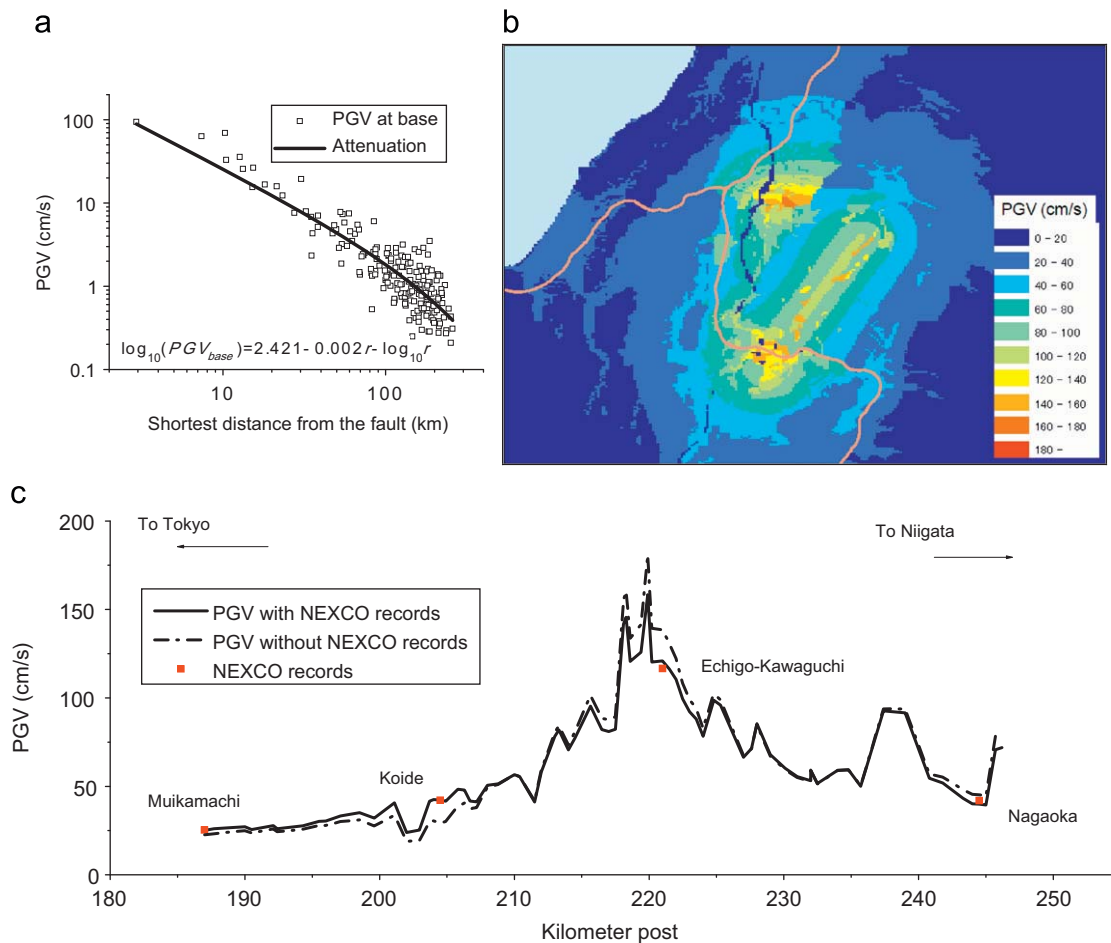


Fig. 6. (a) Attenuation relationship at base rock used as a trend component for Kriging interpolation and (b) estimated distribution PGV for the 2004 Niigata Chuetsu earthquake. (c) PGVs were extracted along the Kan'etsu Expressway.

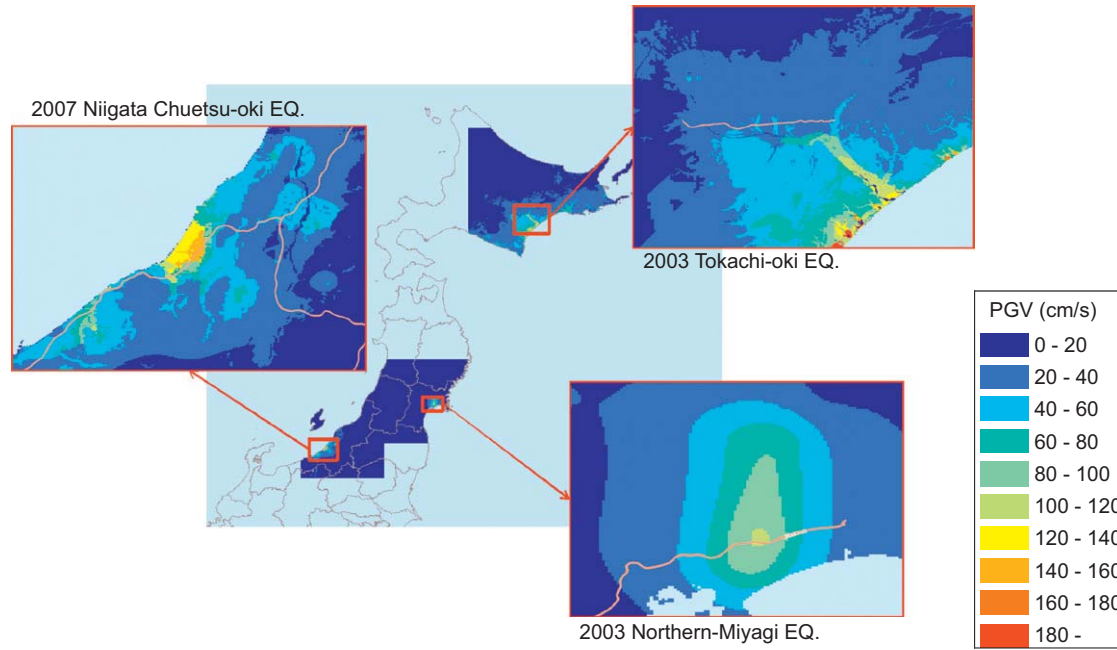


Fig. 7. Estimated PGV distributions for the 2003 Northern-Miyagi, 2003 Tokachi-oki, and 2007 Niigata Chuestu-oki earthquakes. The amplification factors for the 2003 Northern-Miyagi earthquake are not considered because of the limitation of earthquake records near the expressway.

earthquake, the Sanriku expressway, which sustained damage at numerous locations, lies near the epicenter, and the number of seismic observation stations (15 stations) near the expressway was not large enough to use the same methodology. Therefore, the attenuation relationship of the PGV at the ground surface was used as a trend component for Kriging, and the interpolation was then carried out without considering the amplification factor.

4. Construction of fragility curves for expressway embankment

Fig. 8 shows the relationship between the PGV and damage to the expressway embankment for the four earthquakes. The embankment damages are plotted to show the damage levels (Table 1). Damage to side slopes and roadways was observed along embankment sections of expressways. The embankment sections were detected based on cross-sectional drawings along the expressways. Although both roadways and side slopes sustained damage, the damage dataset following the 2007 Niigata Chuetsu-oki earthquake included only damage to roadways. In addition, not all of the minor damage was listed in the dataset.

Table 2 is derived based on the results shown in Fig. 8. Table 2 shows the number of damage incidents to expressway embankments after the four earthquakes. The average PGV in Table 2 shows the mean value along the embankment sections, and the damage to roadways and side slopes are combined. The fragility curves for expressway embankments are constructed based on Table 2. The damage ratio (number of damage incidents per km) of an expressway embankment, P , is assumed to be as follows:

$$P = C\Phi((\ln PGV - \lambda)/\zeta) \quad (6)$$

where $\Phi(x)$ is the cumulative distribution function of the standard normal distribution, and λ , ζ , and C are the constants determined by regression analysis. Using the log-normal distribution multiplied by a constant, C , only three parameters need be

determined in order to evaluate the lower limit of the PGV to cause damage and the upper limit of the damage ratio.

Non-linear regression analysis was performed in order to determine the three parameters in Eq. (6). The error term, ε , shown in Eq. (7) was minimized based on a quasi-Newton method:

$$\varepsilon = \sum (P_R - P)^2 w \quad (7)$$

where P_R is the actual damage ratio of the expressway embankment and w is the length of embankment section of the expressway. Fig. 9 illustrates the fragility curves of expressway embankment constructed in the present study, and Table 3 shows the parameters for fragility curves. Two fragility curves are drawn in Fig. 9. One is for major damage of levels A and B that affects the serviceability of ordinary traffic, and the other is for all damage to expressway embankments. To construct the fragility curve for all of the damage, the dataset after the 2007 Niigata Chuestu-oki earthquake is not considered because not all of the minor damage of levels C and D is listed. As shown in the figure, the number of major damage incidents is approximately 0.1 per kilometer when the PGV shows 47.5 cm/s and the maximum number of damage incidents per kilometer is approximately 3.2. When the PGV is 21.0 cm/s, the number of minor damage incidents to the expressway embankment is approximately 0.1 per kilometer. The saturation of the damage density for major damage is observed in Fig. 9 while the damage ratios including minor damage incidents increase with respect to the PGV. The sites where major damages to embankment occur result from the complexity of the geological and topographical effects and the seismic intensity. Therefore, the number of major damage incidents per kilometer might have the upper limit even under the large PGVs.

5. Applicability of fragility curves with respect to the embankment height

The applicability of fragility curves constructed in this study is discussed from the viewpoint of the height of the embankment.

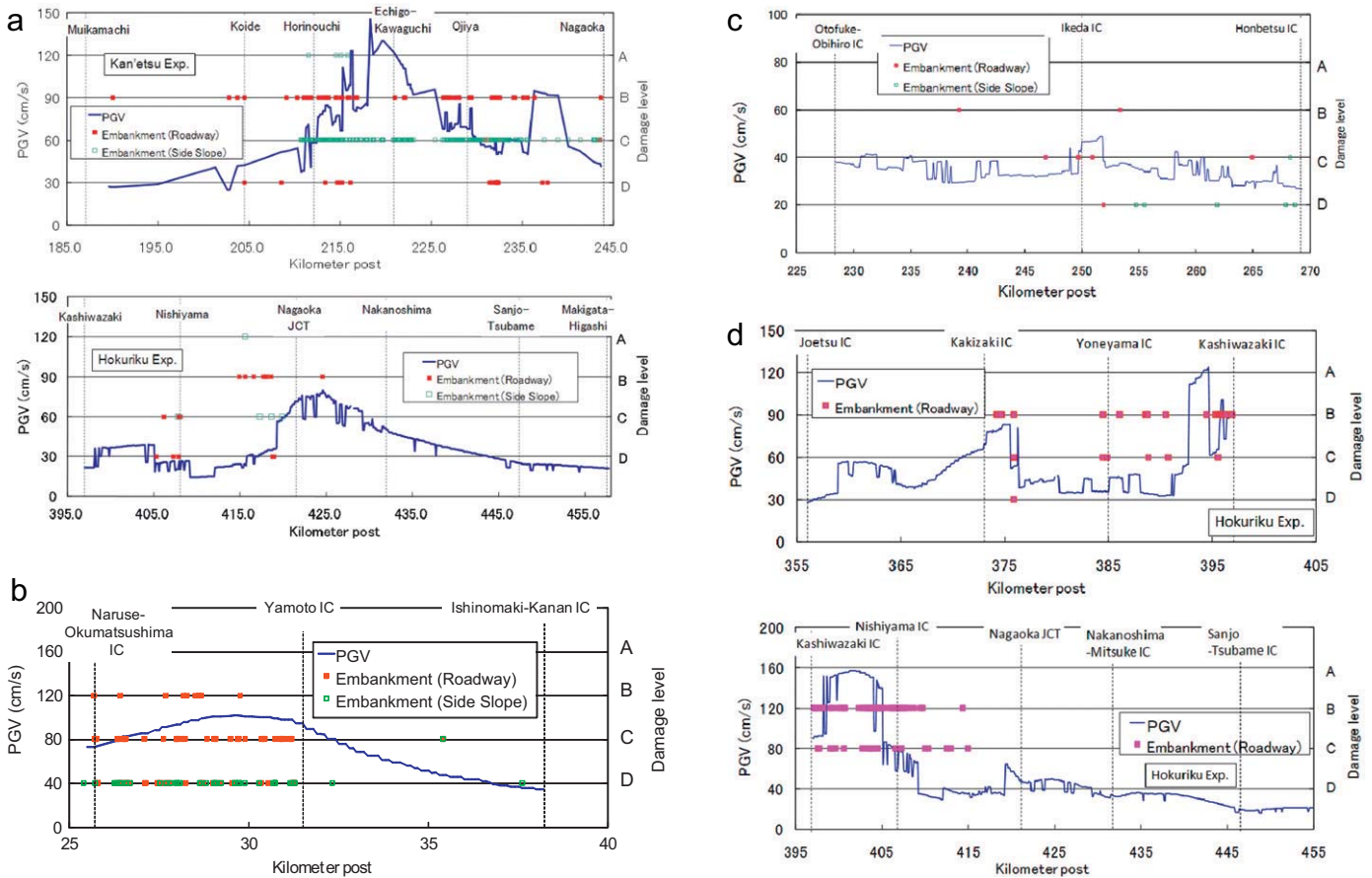


Fig. 8. (1) Relationships between the peak ground velocity and damage to expressway embankments for the (a) 2004 Niigata Chuetsu and (b) 2003 Northern-Miyagi earthquakes. (2) Relationships between the peak ground velocity and damage to expressway embankments for the (c) 2003 Tokachi-oki and (d) 2007 Niigata Chuetsu-oki earthquakes.

The input ground motion to the expressway embankment might be amplified by the response characteristics of the embankment. Since the PGV distributions estimated in the present study represent the input ground motion indices to the embankment, the applicability of the obtained results should be defined properly.

The fragility curves were obtained following the recent four earthquakes. The damage dataset consisted primarily of the damage to the Kan'etsu and Hokuriku Expressways in Niigata Prefecture because two out of the four earthquakes occurred in Niigata. Therefore, the differences in height between the original ground level and the road surface were digitized at 0.1 km intervals along the expressways.

Fig. 10 shows the difference in height and the damage and corresponding damage levels after these two earthquakes. Fig. 11 shows the frequencies of embankment height in Fig. 10 and those associated with damages to embankments following the 2004 Niigata Chuetsu and 2007 Niigata Chuetsu-oki earthquakes. As shown in Figs. 10 and 11, the damage occurrence rate seems to be uniform with respect to the height of embankment. For the Kan'etsu Expressway, numerous damage incidents occurred between 210 and 220 KP, where a repetition of cut-land and fill-land is observed. Generally, the characteristics of seismic responses differ from cut-land to fill-land. These differences might result in the concentration of seismically induced damage.

Although the effects of embankment height on the possibility of damage occurrences were difficult to reveal from the damage dataset used in this study, the amplifications of ground motion

due to the embankment should be properly considered in a future study. Since the most of the damages considered in this study were generated in the embankment sections with the height of 5–10 m, the fragility curves obtained in the present study are applicable to embankments having heights of approximately 5–10 m. Although the boundary of the cut-land and fill-land might be responsible for increased damage to soil structure, further research is necessary in order to confirm this hypothesis.

6. Conclusions

In the present study, the fragility curves of the expressway embankment were constructed using actual damage data of expressways obtained following the 2003 Northern-Miyagi, 2003 Tokachi-oki, 2004 Niigata Chuetsu, and 2007 Niigata Chuetsu-oki earthquakes. To achieve the objectives of the present study, the spatial distributions of PGV were estimated based on a V_s^{30} distribution map of Japan and seismic motion records.

The log-normal distribution multiplied by a constant is adopted as a function to construct the fragility curves. The lower limit of PGV at which damage occurs and the upper limit of the damage ratio can be estimated following this function. According to the fragility curves, major damage that disrupts ordinary traffic on the expressway might occur when the PGV exceeds approximately 45.0 cm/s.

Table 2

Number of damage incidents to expressway embankments after (a) the 2004 Niigata Chuetsu, (b) the 2003 Northern-Miyagi, (c) the 2003 Tokachi-oki, and (d) the 2007 Niigata Chuetsu-oki earthquakes.

PGV (cm/s)	Average PGV (cm/s)	A	B	C	D	Length (km)
(a)						
–30	24.1	1	5	11	4	28.5
30–40	35.3	0	5	18	2	21.8
40–50	44	0	4	14	1	10
50–60	54.9	0	12	110	11	13.7
60–70	66	1	9	52	1	6
70–80	74.6	2	10	43	2	6.8
80–100	91.1	1	15	71	3	6.7
100–	122.1	0	3	40	1	1.9
Total	–	5	63	359	25	95.4
(b)						
–75	50.2	0	1	1	6	5.6
75–85	80.5	0	3	5	17	1.3
85–95	90.2	0	1	8	16	1.5
95–	99.6	0	5	11	43	2.4
Total	–	0	10	25	82	10.8
(c)						
25–35	30.7	0	1	4	4	21.4
35–	38.6	0	1	1	2	11.6
Total	–	0	2	5	6	33
PGV (cm/s)	Average PGV (cm/s)	A	B	C ^a	D ^a	Length (km)
(d)						
–40	29.1	0	10	9	0	59.6
40–50	45.7	0	3	0	0	11.6
50–60	55.2	0	3	2	1	7.3
60–90	75.4	0	41	4	0	8.4
90–140	114.4	0	23	5	0	4
140–160	148.7	0	17	6	0	5.3
Total	–	0	97	26	1	96.2

^a Not all of the damage has been properly recorded.

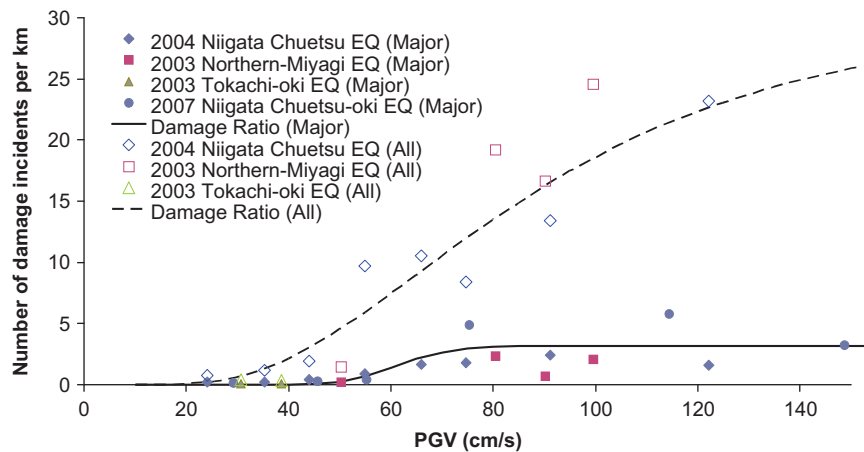


Fig. 9. Two fragility curves of expressway embankments derived in the present study. One is for major damage that affects the serviceability of traffic, and the other is for all damage to expressway embankments.

Table 3

Parameters for fragility curves determined by non-linear regression analysis.

Parameter	ζ	λ	C
Major damage	0.14	4.12	3.19
All damage	0.52	4.45	30.0

The fragility curves were obtained based on four earthquake datasets. Two of the four earthquakes occurred in Niigata Prefecture, and damage to the Kan'etsu and Hokuriku Expressways

was observed. In order to evaluate the applicability of the fragility curves, the height of the expressway embankment was considered. On the whole, the fragility curves obtained in the present study are applicable to embankments having heights of approximately 5–10 m. The boundary of the cut-land and fill-land might be responsible for increased damage to soil structure.

The expressway authorities have deployed seismometers along expressways in Japan. Seismic records are used to quickly and properly adjust traffic control devices following an earthquake. The severity of expressway damage can be estimated soon after an earthquake using the fragility curves proposed in the

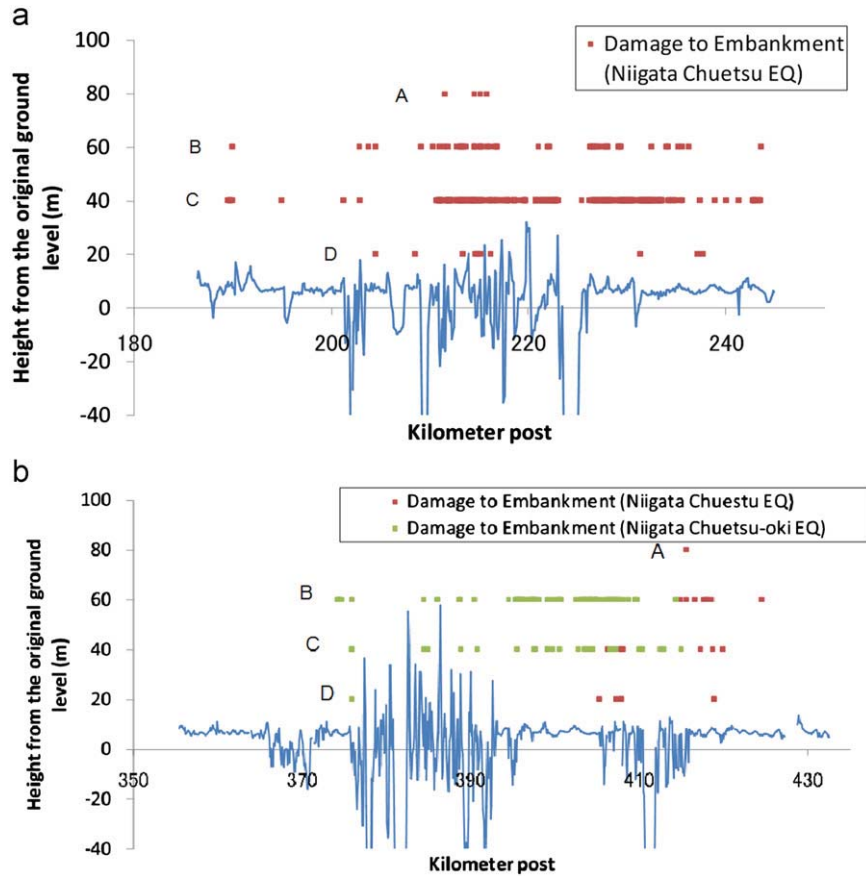


Fig. 10. Height from the original ground level and damage to the embankments of the (a) Kan'etsu and (b) Hokuriku Expressways.

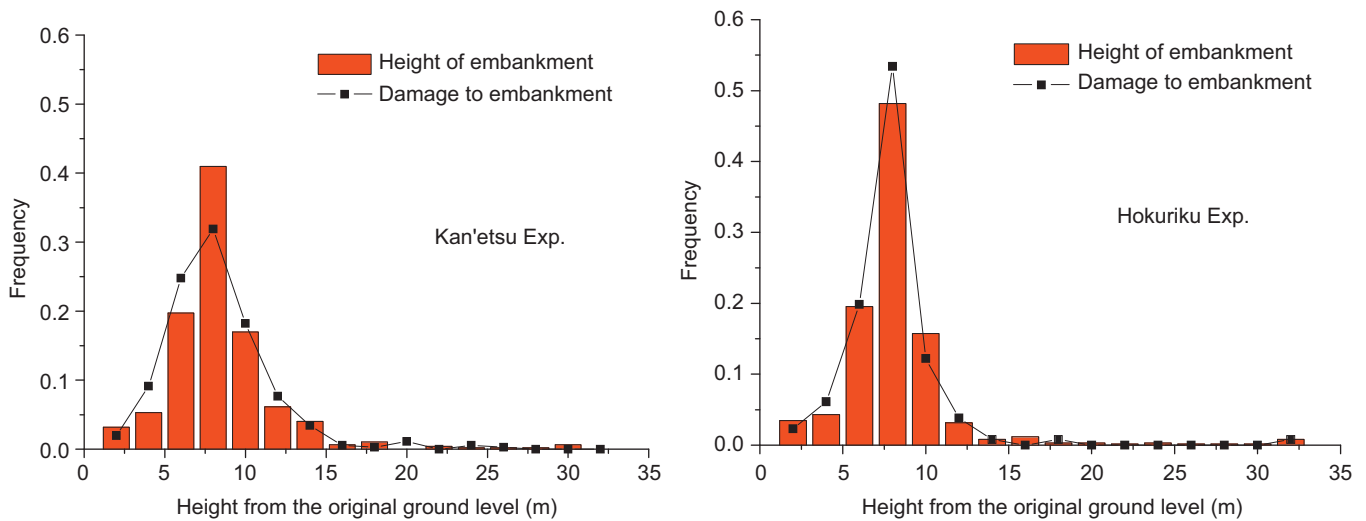


Fig. 11. Frequencies of embankment height for the Kan'etsu and Hokuriku Expressways and those associated with damages to embankments following the 2004 Niigata Chuetsu and the 2007 Niigata Chuetsu-oki earthquakes.

present study. In addition, the fragility curves are useful for preparing countermeasures against future earthquakes.

of Advanced Industrial Science and Technology (AIST) for providing the map of amplification factors of peak ground velocity.

Acknowledgements

The authors appreciate Prof. Kazue Wakamatsu of Kanto Gakuin University and Dr. Masashi Matsuoka of National Institute

References

[1] Japan Meteorological Agency (JMA) <<http://www.jma.go.jp/jma/en/Activities/earthquake.html>>.

- [2] National Research Institute for Earth Science and Disaster Prevention of Japan (NIED) <http://www.kyoshin.bosai.go.jp/index_en.html>.
- [3] Shimizu Y, Yamazaki F, Yasuda S, Towhata I, Suzuki T, Isoyama R, et al. Development of real-time control system for urban gas supply network. *Journal of Geotechnical and Geoenvironmental Engineering, ASCE* 2006;132(2):237–49.
- [4] Maruyama Y, Yamazaki F, Hamada T. Microtremor measurements for the estimation of seismic motion along expressways. In: *Proceedings of the sixth international conference on seismic zonation*, vol. 2, 2000. p. 1361–6.
- [5] Kawashima K. Seismic performance of RC bridge piers in Japan: an evaluation after the 1995 Hyogo-ken Nanbu Earthquake. *Progress in Structural Engineering and Materials* 2000;2:82–91.
- [6] Yamazaki F, Motomura H, Hamada T. Damage assessment of expressway networks in Japan based on seismic monitoring. In: *Proceedings of 12th world conference on earthquake engineering, 2000* (CD-ROM).
- [7] Karim KR, Yamazaki F. Effect of earthquake ground motions on fragility curves of highway bridge piers based on numerical simulation. *Earthquake Engineering & Structural Dynamics* 2001;30(12):1839–56.
- [8] Karim KR, Yamazaki F. A simplified method of constructing fragility curves for highway bridges. *Earthquake Engineering & Structural Dynamics* 2003;32(10):1603–26.
- [9] Mander JB, Basoz N. Seismic fragility curves theory for highway bridges. In: *Proceedings of the fifth US conference on lifeline earthquake engineering, ASCE, TCLEE no. 16, 1999*. p. 31–40.
- [10] Kircher CA, Nassar AA, Kustu O, Holmes WT. Development of building damage functions for earthquake loss estimation. *Earthquake Spectra* 1997;13(4):663–82.
- [11] Basöz N, Kiremidjian A, King S, Law K. Statistical analysis of bridge damage data from the 1994 Northridge, CA, earthquake. *Earthquake Spectra* 1999;15(1):25–54.
- [12] Honda R, Aoi S, Morikawa N, Sekiguchi H, Kunugi T, Fujiwara H. Ground motion and rupture process of the 2004 Mid Niigata prefecture earthquake obtained from strong motion data of K-NET and KiK-net. *Earth Planets and Space* 2005;57:527–32.
- [13] Miyake H, Koketsu K, Hikima K, Shinohara M, Kanazawa T. Source fault of the 2007 Chuetsu-oki, Japan, earthquake. *Bulletin of the Seismological Society of America* 2010;100(1):384–91.
- [14] Joyner WB, Boore DM. Peak horizontal acceleration and velocity from strong-motion records including records from the 1979 Imperial Valley California earthquake. *Bulletin of the Seismological Society of America* 1981;71:2011–38.
- [15] Fukushima Y, Tanaka T. A new attenuation relation for peak horizontal acceleration of strong ground motion in Japan. *Bulletin of the Seismological Society of America* 1990;80(4):757–83.
- [16] Molas GL, Yamazaki F. Attenuation of earthquake ground motion in Japan including deep focus event. *Bulletin of the Seismological Society of America* 1995;85(5):1343–58.
- [17] Building Seismic Safety Council (BSSC). The 2003 HEHRP recommended provisions for the development of seismic regulations for new buildings and other structures, FEMA, Washington, DC, 2003.
- [18] Wills CJ, Petersen M, Bryant WA, Reichle M, Saucedo GJ, Tan S, et al. A site-conditions map for California based on geology and shear-wave velocity. *Bulletin of the Seismological Society of America* 2000;90(6B):S187–S208.
- [19] Matsuoka M, Midorikawa S. GIS-based integrated seismic hazard mapping for a large metropolitan area. In: *Proceedings of the fifth international conference on seismic zonation*, vol. 2, 1995. p. 1334–41.
- [20] Yamazaki F, Wakamatsu K, Onishi J, Shabestari KT. Relationship between geomorphological land classification and soil amplification ratio based on JMA strong motion records. *Journal of Soil Dynamics and Earthquake Engineering* 2000;19:41–53.
- [21] Wakamatsu K, Matsuoka M, Hasegawa K, Kubo S, Sugiura M. GIS-based engineering geomorphologic map for nationwide hazard assessment. In: *Proceedings of the 11th international conference on soil dynamics and earthquake engineering and third international conference on earthquake geotechnical engineering*, vol. 1, 2004. p. 879–86.
- [22] Matsuoka M, Wakamatsu K, Fujimoto K, Midorikawa S. Average Shear-wave velocity mapping using Japan engineering geomorphologic classification map. *Journal of Structural Engineering and Earthquake Engineering, Japan Society of Civil Engineers* 2006;23(1):57s–68s.
- [23] Fujimoto K, Midorikawa S. Empirical estimates of site amplification factor from strong-motion records at nearby station pairs. In: *Proceedings of the 1st European conference on earthquake engineering and seismology, 2006* (Paper no. 251).
- [24] Cressie N. *Statistics for spatial data*. Wiley; 1993.
- [25] Shabestari KT, Yamazaki F, Saita J, Matsuoka M. Estimation of the spatial distribution of ground motion parameters for two recent earthquakes in Japan. *Tectonophysics* 2004;390:193–204.
- [26] Shabestari KT, Yamazaki F. Attenuation relation of strong ground motion indices using K-NET records. In: *Proceedings of the 25th JSCE earthquake engineering symposium*, vol. 1, 1999. p. 137–40.
- [27] Tamura I, Yamazaki F, Shabestari KT. Relationship between the average S-wave velocity and site amplification ratio using K-NET records. In: *Proceedings of the sixth international conference on seismic zonation*, 2000. p. 447–52.
- [28] Geographical Survey Institute (GSI) <<http://www.gsi.go.jp/ENGLISH/index.html>>.